IMA Journal of Numerical Analysis (2026) **00**, 1–25
https://doi.org/10.1093/imanum/draf138

Quadrature formulas from rational approximations

ANDREW HORNING
Department of Mathematical Sciences, Rensselaer Polytechnic Institute, Troy, NY 12180, USA

AND

LLOYD N. TREFETHEN*
School of Engineering and Applied Sciences, Harvard University, Cambridge, MA 02138, USA
*Corresponding author: trefethen@maths.ox.ac.uk

[Received on 11 July 2025; revised on 6 November 2025]

In memory of Nick Higham (1961-2024)

It is shown that quadrature formulas in many different applications can be derived from rational approximation of the Cauchy transform of a weight function. Since rational approximation is now a routine technology, this provides an easy new method to derive all kinds of quadrature formulas as well as fundamental insight into the mathematics of quadrature. Intervals or curves of quadrature nodes correspond to near-optimal branch cuts of the Cauchy transform.

Keywords: rational approximation; quadrature; AAA algorithm; Cauchy transform.

1. Introduction

Quadrature formulas are used across scientific computing, and in numerical linear algebra, they have become an important tool for reducing large-scale eigenvalue and matrix function problems to small sets of matrix solves (Goedecker, 1999; Sakurai & Sugiura, 2003; Hale *et al.*, 2008; Polizzi, 2009; Beyn, 2012; Güttel *et al.*, 2015; Güttel & Tisseur, 2017; El-Guide *et al.*, 2020; Colbrook, 2022; Brennan *et al.*, 2023; Bruno *et al.*, 2024; Horning & Gerlach, 2024; Colbrook & Townsend, 2025). Traditionally, they are derived and analyzed on a case-by-case basis. For one example, Gauss quadrature is connected with the theory of orthogonal polynomials (Gautschi, 2004). For another, the exponentially convergent periodic trapezoidal rule is analyzed by discrete Fourier analysis or estimation of contour integrals (Trefethen & Weideman, 2014). More complicated quadrature problems are reduced to known ones such as these with the aid of conformal maps (Weideman & Trefethen, 2007; Hale & Trefethen, 2008; Hale & Tee, 2009; Güttel & Tisseur, 2017), as in the 'three Nicks' paper by Nick Higham, Nick Hale and the second author (Hale *et al.*, 2008) (see Fig. 15).

In this article we show how quadrature formulas can be generated with very little effort by rational approximation, often approximation of functions with a 'sign(z)' or 'Zolotarev' flavor (Istace & Thiran, 1995; Trefethen & Wilber, 2025). The quadrature nodes are the poles of the rational function, delineating an approximate branch cut on a real interval or a complex contour, and the quadrature weights are the residues. This gives new insight into the mathematics of quadrature formulas. Until recently, there would have been few computational implications, because computation of rational approximations was a difficult problem, but with the appearance of the AAA (adaptive Antoulas-Anderson) algorithm in 2018 (Nakatsukasa *et al.*, 2018; Nakatsukasa & Trefethen, 2025), together with the AAA-Lawson

enhancement to upgrade near-best to best (Nakatsukasa & Trefethen, 2020), it has become routine. The Chebfun code `aaa.m`, which runs in MATLAB or Octave (Driscoll *et al.*, 2014), is used for the examples of this paper, and AAA implementations are also available in Julia (Driscoll, 2023), SciPy (Virtanen *et al.*, 2020) and MathWorks toolboxes (MathWorks, 2024). More recently, another rational approximation algorithm due to Salazar Celis, based on Thiele continued fractions rather than barycentric representations, has also shown great promise (Driscoll, 2023; Salazar Celis, 2024; Driscoll & Zhou, 2025).

Section 2 lays out the mathematics of the connection between rational approximation and quadrature, and Sections 3–7 and 9–10 apply these ideas to seven established quadrature problems, with Section 8 summarizing certain necessary approximation matters related to Zolotarev. In each case, we first apply the rational approximation idea to a standard configuration, and then we show how it can be modified to derive a quadrature formula for a variant problem. Section 11 explains how our quadrature formulas can be interpreted as computing exact integrals of certain rational interpolants, and Section 12 closes the paper with a discussion.

We must say a word about our personal 'journey'. Once the schema of Section 2 became clear, it simply amazed us how, for one problem after another, we were able to use it to reproduce, with a fraction of a second of computing time, results won previously by careful analysis:

Figure 3: see Fig. 4.1 of Hale & Trefethen (2008),
Figure 4: see Fig. 1 of Tee & Trefethen (2006),
Figure 5: see Fig. 2.3 of Hale & Tee (2009),
Figure 9: see Fig. 3 of Deaño & Huybrechs (2009),
Figure 10: see Fig. 4.3 of Trefethen *et al.* (2006),
Figure 11: see Fig. 1 of Weideman & Trefethen (2007),
Figure 13: see Fig. 2 of Austin *et al.* (2014),
Figure 16: see Fig. 2 of Hale *et al.* (2008).

2. Mathematics of the approximation–quadrature connection

As on the left in Fig. 1, let γ be a Jordan arc in the complex plane $\mathbb{C}$, that is, the image of $[-1,1]$ under a real or complex homeomorphism. The simplest example is $[-1,1]$ itself. Let $w(z)$ be an integrable weight function defined on γ, and suppose we are interested in approximating the integral

$$I = \int_\gamma f(z)\, w(z)\, dz. \tag{2.1}$$

Assume f is analytic in the closure of a Jordan region Ω containing γ, bounded by a Jordan curve Γ. By the Cauchy integral formula, we have

$$I = \int_\gamma \frac{1}{2\pi i} \left[\int_\Gamma \frac{f(s)\, ds}{s - z} \right] w(z)\, dz, \tag{2.2}$$

hence by exchanging orders of integration,

$$I = \int_\Gamma f(s) \left[\frac{1}{2\pi i} \int_\gamma \frac{w(z)\, dz}{s - z} \right] ds. \tag{2.3}$$

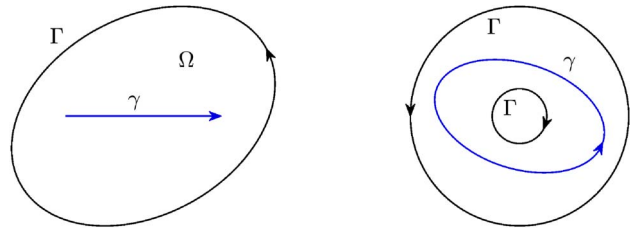

FIG. 1. On the left, sketch of an integration arc γ and a surrounding contour Γ in the complex plane. On the right, the analogous configuration for a closed integration contour γ.

Let $\mathcal{C}(s)$ denote the function in square brackets, the *Cauchy transform* of w,

$$\mathcal{C}(s) = \frac{1}{2\pi i} \int_\gamma \frac{w(z)\,dz}{s - z}, \tag{2.4}$$

which is analytic throughout $(\mathbb{C} \cup \{\infty\}) \backslash \gamma$. (With a different normalization this is also called the *Stieltjes transform.*) Then (2.3) becomes

$$I = \int_\Gamma f(s)\,\mathcal{C}(s)\,ds, \tag{2.5}$$

and thus we have converted a real or complex integral over the arc γ to a complex contour integral over the enclosing contour Γ. Now suppose that r_n is a rational function of degree n that approximates $2\pi i \mathcal{C}$ on Γ. (A rational function of degree n is one that can be written as the ratio of two polynomials of degree at most n.) Then (2.5) suggests approximating I by

$$I_n = \frac{1}{2\pi i} \int_\Gamma f(s)\,r_n(s)\,ds. \tag{2.6}$$

Assume the poles of r_n are n distinct finite numbers $z_1, \ldots, z_n$,[1] so r_n can be written

$$r_n(s) = c_\infty + \sum_{k=1}^{n} \frac{c_k}{s - z_k}, \tag{2.7}$$

where $c_\infty = r_n(\infty)$ and c_k is the residue of r_n at z_k. (In practice, c_∞ is extremely close to zero because of (2.4), and one may subtract off this constant or use a modified AAA algorithm to force an exact zero value at ∞; see Section 11 and (Nakatsukasa & Trefethen, 2025, sec. 32).) Then, assuming all the poles are enclosed by Γ, residue calculus converts (2.6) to

$$I_n = \sum_{k=1}^{n} c_k f(z_k). \tag{2.8}$$

[1] Rational approximations with higher-order poles are possible, in principle, and they can be represented in the barycentric form that is the basis of the AAA algorithm. In numerical practice, however, poles always come out simple, with a double pole in an underlying function, for example, being approximated by a pair of simple poles with large residues. Although problematic examples could perhaps be constructed, we have not seen difficulties in practice.

This is our quadrature approximation to the integral I. If

$$\|2\pi i\mathcal{C} - r_n\|_\Gamma \le \varepsilon, \tag{2.9}$$

where $\|\cdot\|_\Gamma$ is the ∞-norm on Γ, then by (2.5) and (2.6),

$$|I - I_n| \le \frac{\varepsilon}{2\pi}\,|\Gamma|\,\|f\|_\Gamma, \tag{2.10}$$

where $|\Gamma|$ is the arc length of Γ. If $|\Gamma|$ is large or infinite, it is often possible to remove this factor while replacing $\|\mathcal{C} - r_n\|_\Gamma$ or $\|f\|_\Gamma$ by the corresponding 1-norm.

The same reasoning just outlined also applies if γ is a closed Jordan contour, that is, a complex homeomorphism of the unit circle. All that changes now is that for Γ to 'enclose' γ, it should consist of two Jordan contours, one inside γ and the other outside, as sketched on the right in Figure 1.

3. Application 1: Gauss–Legendre quadrature

The most basic quadrature problem is integration of a function f over the interval $\gamma = [-1, 1]$ with weight function $w(z) = 1$:

$$I = \int_{-1}^{1} f(z)\,dz. \tag{3.1}$$

This is the original setting of Gauss quadrature, which is also called Gauss–Legendre quadrature to distinguish it from cases with nonconstant weight functions (Sections 5 and 6). Gauss derived his method by rational approximation of the Cauchy transform (2.4) of $w(z) = 1$ on $[-1, 1]$, which is $\mathcal{C}(s) = (2\pi i)^{-1}\log((s+1)/(s-1))$ (Gauss, 1814; Gautschi, 1981). The only difference from the mathematics of the last section is that he used a Padé approximation at $s = \infty$ rather than an approximation over a contour Γ. This was before Cauchy integrals and long before Padé, so Gauss's formulation, emphasizing continued fractions and hypergeometric series, is quite different from ours.

To illustrate the derivation of essentially the same quadrature formulas via rational approximation on a contour Γ, consider the test integrand $f(z) = 1/(1 + 20z^2)$, which is analytic in the complex z-plane except at $z = \pm i/\sqrt{20}$. Motivated by standard results in approximation and quadrature, let us design a quadrature rule for functions analytic inside the Bernstein ellipse Γ (ellipse with foci ± 1) passing through these two points (Trefethen, 2019). In the standard notation, this is the ellipse with parameter $\rho = 1/\sqrt{20} + \sqrt{21/20} \approx 1.248$ (sum of semiminor and semimajor axis lengths). For AAA approximation, the degree n can be prescribed, or a tolerance for (2.9) can be specified so that n is determined adaptively. Here we compute an approximation $r_n(s) \approx 2\pi i\mathcal{C}(s)$ of degree $n = 20$ in about 0.05 s on a laptop with the code

```
rho = 1/sqrt(20) + sqrt(21/20);
c = rho*exp(2i*pi*(1:200)'/200);
S = (c+1./c)/2;
C = log((S+1)./(S-1));
[r,pol,res] = aaa(C,S,'degree',20,'sign',1);
```

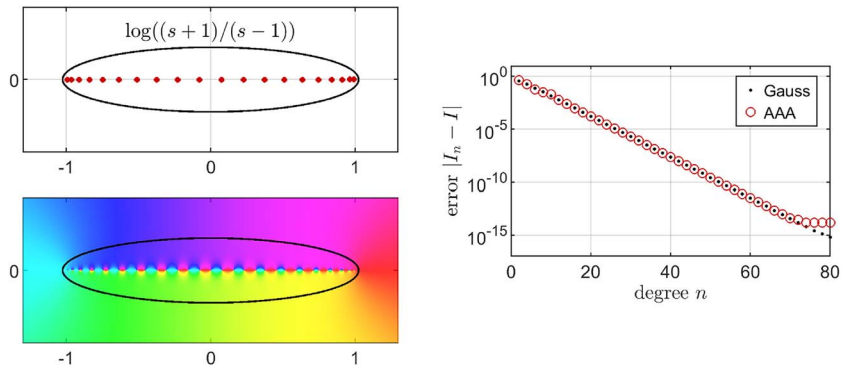

FIG. 2. Quadrature by AAA rational approximation of $2\pi i C(s) = \log((s+1)/(s-1)))$ on the Bernstein ellipse passing through the singularities at $\pm i/\sqrt{20}$ of the test integrand $f(z) = 1/(1+20z^2)$ on $[-1,1]$. The upper-left image shows AAA poles for degree $n = 20$, close to the Gauss quadrature nodes of the same degree, and the lower-left image is a phase portrait of the AAA approximation $r_{20}(z)$ (red for positive real, cyan for negative real (Wegert, 2012)). The right image shows convergence for this integrand as a function of degree n.

(The `'sign'` flag is discussed in Section 8. As for the use of 200 sample points, the discretization details in these computations are usually not important, and one can bypass them by using the alternative continuum AAA algorithm (Driscoll, 2023; Driscoll *et al.*, 2024; Driscoll & Zhou, 2025).) Here and in all our code segments, `S` is a vector of sample points s_k on Γ and `C` is a corresponding vector of values $2\pi i C(s_k)$. The three outputs from `aaa` are `r`, a function handle for the rational approximation, and `pol` and `res`, n-vectors of its poles and corresponding residues. Figure 2 shows that the poles look like Gauss quadrature points, and one can check that the weights are also close to Gauss weights. Following (2.8), a quadrature result can be obtained with

```
f = @(z) 1./(1+20*z.^2);
In = res.'*f(pol)
```

and this gives `In` $\approx 0.603943 - 0.00000002i$, matching the exact value $I \approx 0.604100$ with an error of $1.6 \cdot 10^{-4}$.

In this and other experiments of this paper, the nodes and weights and computed integrals are all slightly complex even when one would expect them to be real. This is because the Chebfun implementation of AAA does not enforce real symmetry, although this can be fixed, as is done in some other implementations such as the `rational` code in the MathWorks RF Toolbox (MathWorks, 2024). With such an adjustment, real symmetric problems give exactly real results.

The phase portrait in Fig. 2 shows a clear approximation to the branch cut of $\log((s+1)/(s-1))$ along $[-1,1]$, and the plot on the right shows that the convergence as a function of n closely matches that of Gauss quadrature. Here as in our later plots, convergence eventually stagnates for reasons related to rounding errors, which we do not attempt to analyze.

For a variant problem that Carl Gauss could not have handled, we start from the observation that although Gauss quadrature is commonly regarded as optimal, this is only true in specialized senses. Gauss quadrature is the unique n-point quadrature formula that integrates polynomials of degree $\le 2n-1$ exactly, and relatedly, it is optimal in a certain sense for integrands analytic in a Bernstein ellipse, which is a natural domain for polynomials. For integration of functions known to be analytic in domains other than ellipses, however, it is suboptimal (Bakhvalov, 1967; Trefethen, 2022). A more natural assumption

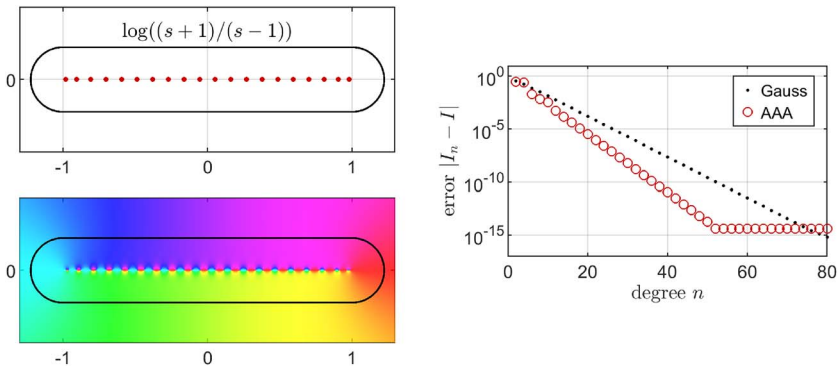

FIG. 3. Variant of Fig. 2 in which $\log((s+1)/(s-1))$ is approximated on an ε-neighborhood of $[-1,1]$ rather than a Bernstein ellipse. For the same test integrand as before, the convergence is now faster by a factor of about $\pi/2$, and the quadrature nodes are more evenly spaced.

to make about an integrand may sometimes be that it is analytic in an ε-neighborhood of $[-1,1]$, and in Hale & Trefethen (2008), quadrature formulas were constructed for such classes based on conformal transplantation of a Bernstein ellipse. (One could equally well consider a rectangular or other domain.) With rational approximation, we can get the same effect without the conformal mapping by changing the approximation contour Γ from an ellipse to a stadium, like this:

```
ep = 1/sqrt(20);
S = [-1i*ep+linspace(-1,1,100)'; 1+ep*exp(1i*pi*(-49:49)'/100)];
S = [S; -S];
```

Figure 3 shows that for the same integrand $f(z) = 1/(1+20z^2)$ as before, the convergence is now faster by a factor of about $\pi/2$. Compare Fig. 3.4 of Hale & Trefethen (2008) and Fig. 4.1 of Trefethen (2022). Perhaps more importantly, the quadrature nodes are more evenly spaced, a property that can be advantageous in time-stepping applications when there are CFL stability constraints (Kosloff & Tal-Ezer, 1993). The quadrature weights are also closer to uniform.[2]

Regarding quadrature weights, in classical Gauss-type cases the nodes are real and the weights are positive. When we treat such problems by AAA approximation, we do not impose exact symmetry, and both the nodes and weights come out slightly complex. For example, with the degree 20 approximation of Fig. 3, the absolute values of the imaginary parts of the poles are less than $5.1 \cdot 10^{-6}$ and those of the weights are less than $1.8 \cdot 10^{-6}$. It is clear the weights would be positive if the approximation imposed symmetry. At present, we do not have any theory, however, to quantify how generally this must be true with weights of quadrature formulas obtained from rational approximation.

4. Application 2: Quadrature with nearby singularities

A theme of this article is that transplantation by conformal maps has been a tool often used for enhancing accuracy of integrals. A remarkable success in this direction was due to Wynn Tee in his construction

[2] The reader may be puzzled how one can have nearly equispaced nodes without coming up against the Runge phenomenon of exponentially large weights with alternating signs. The explanation is that that is a phenomenon of polynomial interpolation, whereas here, the quadrature rule is implicitly interpolating by rational functions (Hale & Trefethen, 2008). See section 11.

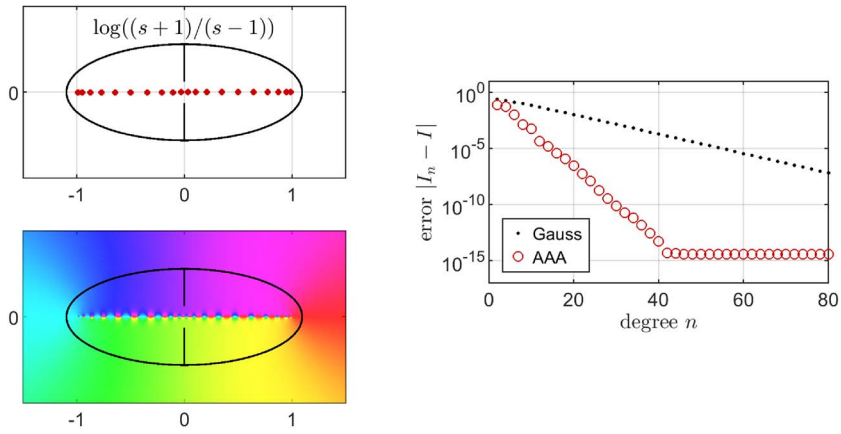

FIG. 4. Construction of a quadrature formula for an integrand with a conjugate pair of singularities near $[-1, 1]$, motivated by Tee & Trefethen (2006). The test integrand is $1/(1 + 100z^2)$.

of numerical methods for time-dependent blow-up and shock PDE problems (Tee & Trefethen, 2006). (The second author was the junior partner in this work.) Using an adapted spectral spatial grid with as few as 56 points, Tee was able to resolve the solution to $u_t = u_{xx} + e^u$ on $[-1, 1]$ with homogeneous initial and boundary conditions up to a time within 10^{-8} of the blowup time of $t_c \approx 3.54466459$. Tee's method can be described with reference to Fig. 4. The difficulty in these problems is a pair of complex singularities approaching the real axis as $t \to t_c$, for singularities at distance ε would ordinarily require a grid of $O(\varepsilon^{-1})$ points. If the singularities are regarded as the ends of branch cut slits in the complex plane, however, he showed that a conformal transplantation can be used to send them far away, improving $O(\varepsilon^{-1})$ to $O(|\log \varepsilon|)$.

All this required careful analysis of conformal maps, but in the experiment shown in the figure, we have achieved the same effect (for quadrature rather than PDEs) by rational approximation. The same Cauchy transform as in the last section, $2\pi i\mathcal{C}(s) = \log((s + 1)/(s - 1))$, is now approximated on a Bernstein ellipse to which a conjugate pair of slits extending to $\pm 0.1i$ have been added. For the test integrand $f(z) = 1/(1 + 100z^2)$, whose singularities lie at the ends of the slits, one sees about a fivefold speedup over Gauss–Legendre quadrature. Closer singularities would amplify the effect. In Tee's paper he estimates the singularity positions on the fly with Chebyshev–Padé approximation, which we would now propose to replace by AAA.

After the completion of Tee & Trefethen (2006), Hale & Tee (2009) generalized Tee's method to problems with multiple conjugate pairs of singularities near the approximation interval. Their generalization was again highly successful, but required expert Schwarz–Christoffel mapping. As a variant problem for this section, Fig. 5 shows the same kind of improvement as in Fig. 4 for a problem with several singularities. To highlight the flexibility of the method, we have chosen a complex integrand whose singularities do not lie in conjugate pairs, namely $f(z) = \log([z - .01i]i) + \log([z - (.5 - .01i)]/i)$. The snaky curve in the figure emphasizes the fact that in general, rational approximation chooses the contour as well as the nodes and weights. The examples of Figs 8–11, 14, 16 and 17 are also notably of this kind. Indeed, near-optimal rational approximations are always choosing a near-optimal contour, and this merely fails to be apparent when the contour is simply a real interval for reasons of symmetry. The reasons for such contour choices are related to potential theory, and the case that has been worked

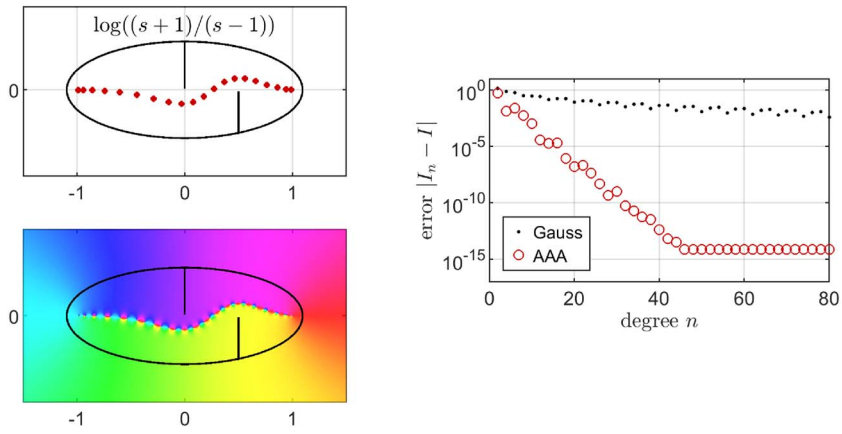

FIG. 5. Variant of Fig. 4 inspired by Hale & Tee (2009) in which there may be several singularities near $[-1,1]$, and not just conjugate pairs. The test integrand is $\log([z-.01i]i)+\log([z-(.5-.01i)]/i)$.

out most fully is that of minimal-capacity curves of poles and zeros arising in Padé approximation of functions with branch points, as investigated by Stahl (1997).

5. Application 3: Singular integrals

The method of Section 2 is straightforward to adapt to a variety of challenging (and interesting!) nonconstant weight functions $w(z)$ in (2.1). The new ingredient is that we need samples from the Cauchy transform of $w(z)$ to feed into AAA. In some special cases, just as for $w(z)=1$ in the last two sections, the Cauchy transform can be determined analytically. In practice, it is convenient to evaluate it numerically on the contour Γ using an adaptive quadrature rule. In this and the next section we demonstrate this approach in two settings: first weakly singular integrals, then highly oscillatory ones.

For the first example, suppose $w(z)$ in (2.1) is integrable but not necessarily smooth or bounded. Numerical methods are often based on adaptive node refinement, analytic expansions, domain mapping, or hybrid schemes that combine these elements (for example, see 'quadrature by expansion' (Klöckner *et al.*, 2013) and references therein). Adaptive refinement may evaluate $f(z)$ many times, while analytic expansions and domain mapping techniques, for maximal efficacy, are derived on a case-by-case basis for different classes of weight functions. However, rational approximation offers the alternative of easy construction of Gauss-like formulas for arbitrary weights. To illustrate, consider the asymmetric Jacobi weight $w(z)=(1+z)^{3/2}(1-z)^{-1/2}$. This weight has algebraic singularities at both endpoints and blows up at the right endpoint. To obtain a quadrature rule with AAA, we compute samples of $2\pi i\mathcal{C}(s)$ along the Bernstein ellipse of Section 3 with Gauss–Kronrod quadrature as implemented in `quadgk` in MATLAB:

```
rho = 1/sqrt(20) + sqrt(21/20);
c = rho*exp(2i*pi*(1:400)/400);
S = (c+1./c)/2;
w = @(z) sqrt(1+z).^3./sqrt(1-z);
C = arrayfun(@(s) quadgk(@(z) w(z)./(s-z),-1,1),S);
[r,pol,res] = aaa(C,S,'degree',20,'sign',1);
```

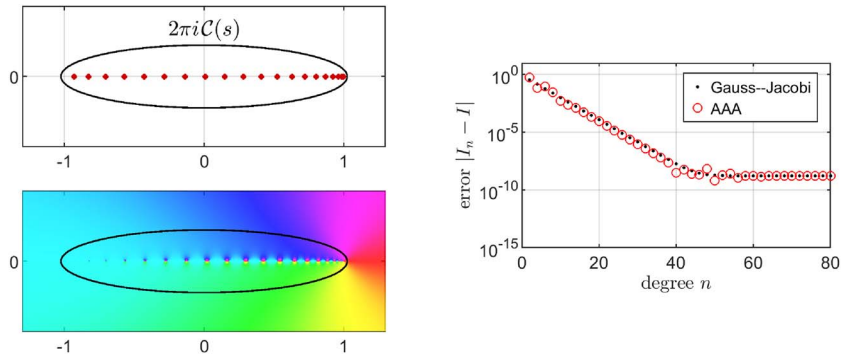

FIG. 6. AAA quadrature for the singular Jacobi weight function $w(z) = (1+z)^{3/2}(1-z)^{-1/2}$. The AAA poles cluster asymmetrically to capture the blow-up at $x = 1$.

For higher-degree rules, one should adjust the default tolerances in `quadgk` to sample $\mathcal{C}(s)$ with sufficient accuracy. For this section, we set both `'AbsTol'` and `'RelTol'` to 10^{-13}. The left panel of Fig. 6 displays the quadrature nodes (poles of $r_n(s) \approx 2\pi i\mathcal{C}(s)$) along with the phase portrait of r_n. The quadrature nodes cluster asymmetrically toward the right endpoint to capture the blow-up of $w(z)$ there, and the phase portrait makes it clear that this is where most of the action is. The Gauss–Jacobi nodes and weights associated with this weight function exhibit similar behavior (not shown). The right panel compares the convergence of AAA quadrature, for the same function $f(z)$ as in Section 3, with that of the Gauss–Jacobi quadrature rule computed with `jacpts` in Chebfun. Clearly, rational approximation has discovered rules that are essentially as effective as Gauss quadrature.

Our variant for this section concerns the nonclassical weight function on $[-1, 1]$ defined by

$$w(z) = \begin{cases} \sqrt{1-z^2} & 0.5 \le |z| \le 1, \\ 0 & \text{otherwise.} \end{cases} \tag{5.1}$$

This weight function is supported on the disjoint intervals $[-1, -0.5]$ and $[0.5, 1]$ and is not differentiable at any of the endpoints. Weight functions supported on disjoint intervals present a common challenge in the computation of response integrals in quantum chemistry and materials science, where points of nondifferentiability at 'band edges' or in the 'bulk bands' are often associated with fascinating physical phenomena (Wallace, 1947; Van Hove, 1953). High-order quadrature schemes must take care to resolve such singularities, which can degrade the convergence of popular 'out-of-the-box' methods like the Kernel Polynomial Method (KPM) (Silver *et al.*, 1996; Weisse *et al.*, 2006).

AAA generates a new quadrature rule for the nonclassical weight function with a single modification to the code above, namely, defining the new weight function. Figure 7 is the analog of Fig. 6 for the new AAA quadrature rule, and one can see that the quadrature nodes are confined to the support of the weight function. (Our data are for even n. Choosing an odd value of n typically leads to an additional pole far from the interval of integration, with a negligible residue.) For this example, one could also design a specialized rule by partitioning the integration domain into $[-1, -0.5]$ and $[0.5, 1]$ and applying different Gauss–Jacobi rules on each subdomain. However, this strategy requires detailed knowledge of the location and type of each singularity. The AAA approach achieves similar performance while only requiring evaluation of the weight function on $[-1, 1]$.

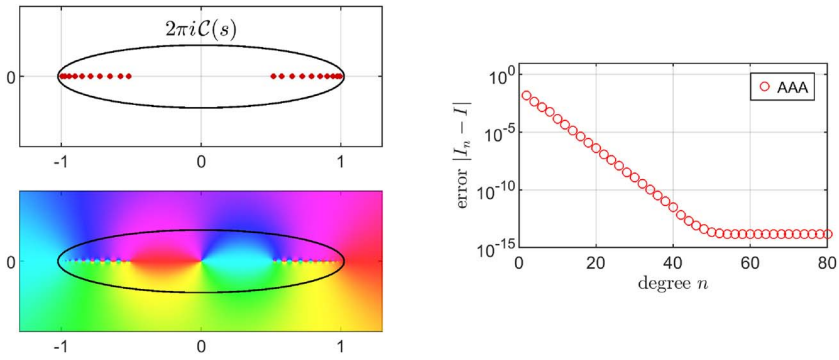

FIG. 7. AAA quadrature for the weight function (5.1). Poles appear only in the portions of $[-1, 1]$ where $w(z)$ is nonzero.

6. Application 4: Oscillatory integrals

For our next application, suppose we want to compute an *oscillatory* integral of the form

$$I = \int_{-1}^{1} f(z) \exp(i\omega g(z))\, dz, \tag{6.1}$$

where $g(z)$ is a smooth *phase function* and ω is a real frequency. Such oscillatory integrals arise in scattering problems and related applications in, e.g., imaging; see Chandler-Wilde *et al.* (2012) and many references therein. Traditional Gauss quadratures require many samples of $f(z)$ when ω is large, as they must satisfy the Nyquist sampling criterion associated with polynomial interpolation of the integrand. More efficient methods, which improve as ω increases, rely on specialized asymptotic expansions that exploit oscillation and cancelation in the integrand (Filon, 1930; Levin, 1982; Deaño *et al.*, 2017). When $g(z)$ is analytic, the key ideas are those of stationary phase, to identify points of dominant contribution, and steepest descent, to identify paths in the complex plane along which the integrand decays exponentially. By deforming the contour off of $[-1, 1]$ along paths of steepest descent through points of stationary phase, one can truncate and apply Gauss quadrature on the deformed integral to derive methods that are convergent and of optimal order as $\omega \to \infty$ (Huybrechs & Vandewalle, 2006; Deaño & Huybrechs, 2009).

Remarkably, AAA approximation of the Cauchy transform of the weight function $w(z) = \exp(i\omega g(z))$ appears to generate quadrature rules of similar structure and similar efficiency. To illustrate, fix $\omega = 25\pi \approx 78.53$ and consider the simplest phase function, $g(z) = z$, corresponding to a band-limited Fourier transform. Since $g'(z) = 1$ is nonvanishing, there are no stationary points, and the dominant contributions to I come from the endpoints. The classical 'two-point' quadratures associated with highly oscillatory integrals approximate I with a weighted combination of f and its derivatives evaluated at the endpoints. For a fresh account with modern developments, see Iserles *et al.* (2006).

Now, as in the previous section, we compute the Cauchy transform of $w(z) = \exp(25\pi iz)$ on the Bernstein ellipse with $\rho = 2$ using `quadgk`. The samples of the Cauchy transform are fed into AAA, which generates a rational approximation of user-specified degree, whose poles and residues become the quadrature nodes and weights. Figure 8 shows that these quadrature nodes cluster densely at the endpoints of the interval. Moreover, they lie along nearly vertical arcs in the upper half-plane, with a slight inclination away from the ellipse. Further experiments (not shown) reveal that when the Cauchy

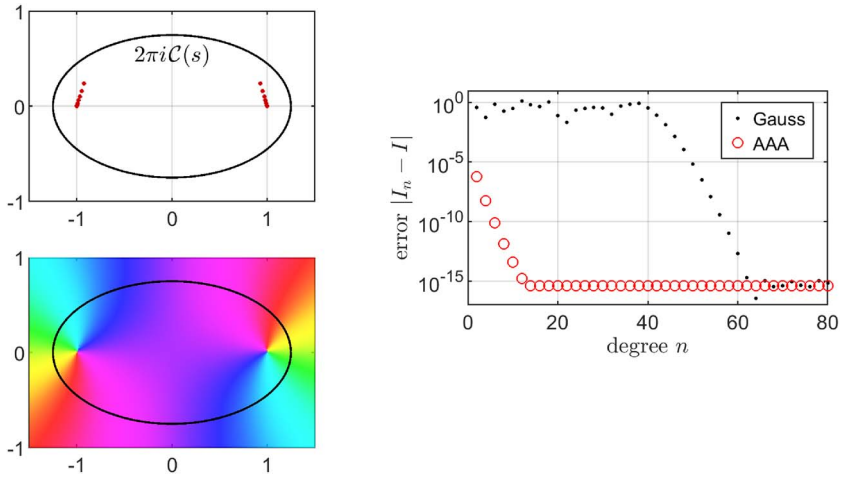

FIG. 8. AAA quadrature for the oscillatory integral in (6.1) with $\omega = 25\pi$ and $g(z) = z$. The quadrature nodes cluster near the endpoints along arcs that are close to paths of steepest descent. The right panel shows convergence for $f(z) = 1/(1 + z^2/4)$ as the degree of the quadrature rule is increased and compares with Gauss–Legendre quadrature.

transform is sampled on a smaller Bernstein ellipse, the nodes crowd inward as if confined to the interior of the ellipse. When the ellipse is made larger, the nodes tend toward vertical lines in the upper half-plane—the paths of steepest descent for this Fourier integral.

For the variant, we consider the phase function $g(z) = z^4$, which has a stationary point of order 3 at $z = 0$. The associated path of steepest descent slices through the origin in the complex plane at an angle of $\pi/8$. Some of the quadrature nodes computed by AAA again cluster at the endpoints, though this is hard to see in Fig. 9: there are three nodes at distances about 0.00132, 0.00732 and 0.02011 above $s = 1$ in the complex plane and three more at the same distances below $s = -1$. More visibly in the plot, there are also 13 nodes distributed evenly along an arc close to the path of steepest descent through $z = 0$. When the Cauchy transform is sampled on a smaller Bernstein ellipse (not shown), the nodes distribute themselves along an arc that is close to the path of steepest descent near the real line but curves away to fit within the ellipse off of the real line.

For both the examples of this section, as well as other related problems, it would be very interesting to investigate more carefully the relationship between quadrature formulas obtained by rational approximation and those associated with steepest descent and Gauss quadrature for complex oscillatory weight functions.

7. Application 5: Hankel contours for inverse Laplace transforms

John Butcher in the 1950s and Alan Talbot in the 1970s introduced the powerful technique of computing inverse Laplace transforms via discretizations of integrals over so-called *Hankel contours,*

$$I = \int_\gamma e^z f(z)\,dz \approx \sum_{k=1}^{n} c_k f(z_k). \tag{7.1}$$

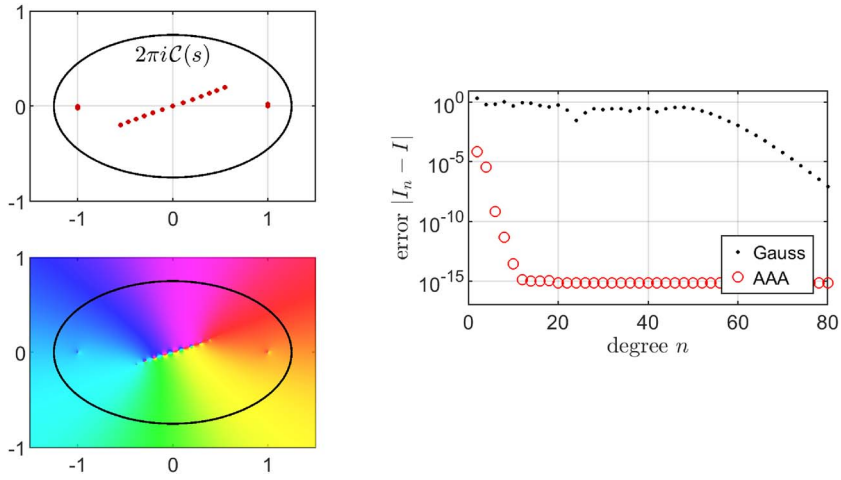

FIG. 9. Same as in Fig. 8 but for the weight function $g(z) = z^4$.

A Hankel contour γ is an infinite arc in the complex plane wrapping around $(-\infty, 0]$ from $-\infty - 0i$ to $-\infty + 0i$ (and thus not precisely a homeomorphism of $[-1, 1]$). Here f is a function analytic in the simplest cases in $\mathbb{C}\backslash(-\infty, 0]$ which may be a scalar for applications to special functions or a large-dimensional matrix function for applications in computational science. Many researchers have worked with such techniques including Gallopoulos, Gavrilyuk, Gil, López-Fernández, Lubich, Luke, Makarov, McLean, Palencia, Saad, Schädle, Schmelzer, Sheen, Sloan, Temme, Thomée and Trefethen, and the one who has investigated them most systematically is Weideman (Trefethen *et al.*, 2006; Weideman & Trefethen, 2007). See these papers and Trefethen & Weideman (2014) for technical details and references.

To address (7.1) by rational approximation, we interpret e^z as a weight function on some Hankel contour γ; exactly which one does not matter. Since e^z is analytic, it follows from (2.4) that the Cauchy transform $\mathcal{C}(s)$ is $-e^s$ for s inside γ and 0 for s outside. To define Γ in a manner consistent with the second image of Fig. 1, we take it to be $\Gamma = (-\infty, 0]$, traversed from left to right along the top and then right to left along the bottom. In principle, Γ should also include an outer boundary on which the value to be matched will be 0. However, this part of Γ does not need to be considered explicitly, as a rational approximation to $-2\pi i e^s$ on $(-\infty, 0]$ will necessarily be ≈ 0 for $s \to \infty$. We can compute an approximation with the code

```
S = -logspace(-3,4,300)';
C = -2i*pi*exp(S);
[r,pol,res] = aaa(C,S,'degree',14);
```

The degree 14 is fixed as the highest possible before reaching machine precision (Trefethen, 2019, chap. 20). Figure 10 shows the very satisfactory result, with poles closely matching those in the papers cited above. A numerical calculation based on another integrand with integral 1,

```
f = @(z) (exp(1)/(2i*pi))./(1+z);
In = res.'*f(pol)
```

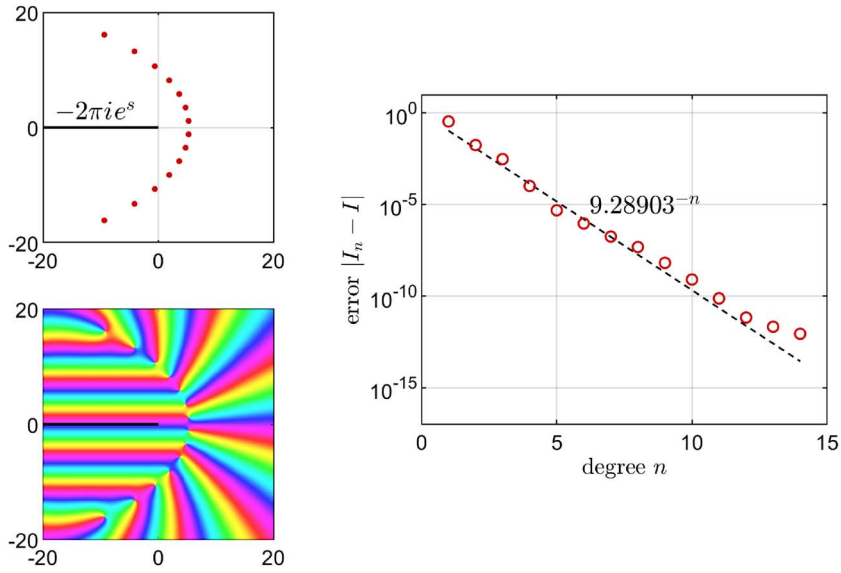

FIG. 10. Evaluation of the inverse Laplace transform by rational approximation following Butcher, Talbot and many later authors. On the left, quadrature poles with $n = 14$, giving 12-digit accuracy for a test problem based on just 7 matrix solves (if real symmetry is exploited). The stripes in the phase portrait match those of e^z to the left of the curve of poles. On the right, convergence as a function of n, matching the optimal rate for best approximation.

gives the result $0.99999999999937 + 0.00000000000003i$ with error $6.3 \cdot 10^{-13}$. The convergence as a function of $n \to \infty$ closely tracks the optimal rate $(9.28903\ldots)^{-n}$ (Trefethen, 2019, Thm. 25.2).

The elegant curve of poles on the left in Fig. 10 echoes similar images to be found in Figs 3.1–3.3 and 4.3 of Trefethen *et al.* (2006), where quadrature formulas are compared based on parabolic, hyperbolic and cotangent ('Talbot') contours as well as true best approximations of e^z on $(-\infty, 0]$. In the first three cases, exponential convergence rates on the orders of 2.85^{-n}, 3.20^{-n} and 3.89^{-n} are obtained, whereas as we see in Fig. 10, rational approximation gives the optimal rate of about 9.29^{-n}. This approximate doubling of the convergence rate, which we think of as the 'Gauss quadrature factor of 2,' arises in many contexts of rational approximation in the difference between estimates obtained from potential theory arguments assuming $n + 1$ interpolation points of a rational approximation and the improved estimates, related to orthogonality, that come when there are $2n + 1$ interpolation points. See the end of Trefethen (2025) for a brief discussion and Rakhmanov (2016) and (Nakatsukasa & Trefethen, 2025, sec. 12) for theorems.

Our variant problem for this section concerns a setting in which it is supposed that the function f, which may be derived from a matrix or operator, is *sectorial,* meaning that it is analytic and satisfies a growth condition outside a wedge in the left half-plane (López-Fernández *et al.*, 2006; Weideman & Trefethen, 2007). A small change in the definition of the approximation domain,

```
S = -logspace(-3,4,300)';
S = [flipud(S)/exp(.333i*pi); S*exp(.333i*pi)];
```

gives the images of Fig. 11, now with the degree increased from $n = 14$ to $n = 20$ since the problem is slightly harder.

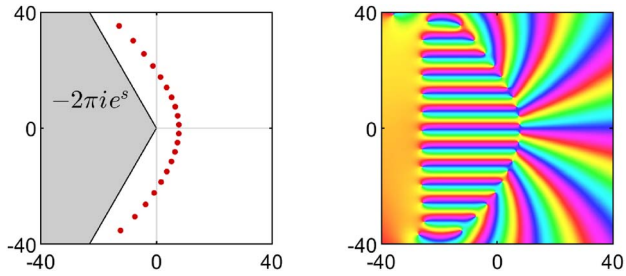

FIG. 11. Variant problem for a sectorial operator as in López-Fernández *et al.* (2006). The reason the stripes terminate at around real part -35 is that e^{-35} is on the order of the accuracy of this approximant, close to machine precision.

8. AAA approximation of sign functions

The last five sections could have been written 5 years ago, based on the AAA and AAA-Lawson algorithms of Nakatsukasa *et al.* (2018) and Nakatsukasa & Trefethen (2020). In the next two sections we will turn to examples involving approximation on two disjoint contours (see the right image of Fig. 1), where a rational approximation is needed to a function with two branches, and here, these original algorithms proved unreliable. However, modifications were introduced in 2024 that make problems of this kind tractable too (Trefethen & Wilber, 2025). These variants are invoked by specifying the `'sign'` and/or `'damping'` options in calls to `aaa`. The first of these adjustments bases the AAA choice of a barycentric weight vector on a weighted blend of all the singular vectors of a Loewner matrix rather than just one, and the second introduces a damping factor in the update formula of the AAA-Lawson iteration. We will not discuss the details here, as they are treated in Trefethen & Wilber (2025) and the topic of this paper is the link from rational approximation to quadrature, not the mechanics of rational approximation.

To illustrate the new capabilities, here is an example adapted from Trefethen & Wilber (2025) of AAA computation of an approximate sign function. Suppose it is desired to find a rational function r_n of degree $n = 20$ that comes as close as possible to taking the values -1 and $+1$ on the two components of the yin-yang domain of Fig. 12. This is an example of 'Zolotarev's 4th problem', also known as the Zolotarev sign problem (Istace & Thiran, 1995; Trefethen & Wilber, 2025). We discretize the domain by 300 points on the boundary of each component.

```
c = exp(1i*pi*(1:100)'/100)/1i;
yin = [-c; conj(1i*c)/2i-.5i; c/2+.5i] - 1/2;
yang = -yin;
S = [yin; yang];
```

No single analytic function can match the values -1 and 1 exactly; there must be a branch cut. Near-best rational approximations mimic this behavior by forming approximate branch cuts out of strings of poles and zeros. The rational approximation is computed in about 0.7 s on a laptop by these commands:

```
C = [-ones(size(yin)); ones(size(yang))];
[r,pol,res,zer] = aaa(C,S,'degree',20,'sign',1);
plot(yin,'-k'), hold on, plot(yang,'-k')
plot(zer,'.g'); plot(pol,'.r');
```

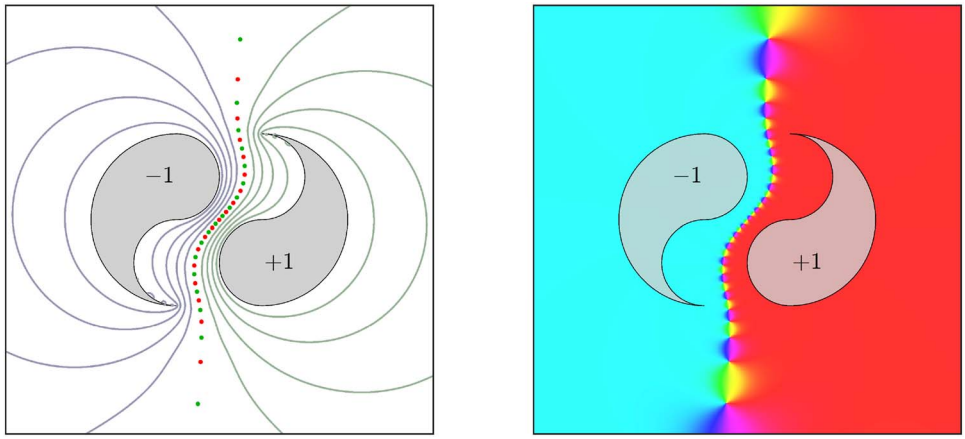

FIG. 12. Degree 20 rational approximation $r_n(s)$ of a sign function on a two-component yin-yang domain in the complex plane. On the left, the domain is shown together with poles (red) and zeros (green) of the rational approximation, defining an approximate branch cut, as well as error contours $|r_n(s) - (\pm 1)| = 10^{-1}, \ldots, 10^{-4}$. On the right, a phase portrait of r_n.

The error contours in the figure can be understood at least approximately—and exactly, in the limit $n \to \infty$—by methods of potential theory (Trefethen, 2025). The potential function in question is generated by positive and negative charges on the two components distributed in a minimal-energy configuration.

The example of Fig. 12 can be regarded as a prototype of the kind of rational approximation needed for applications involving Cauchy integrals over closed contours γ that separate $\mathbb{C}$ into an interior and an exterior region.

9. Application 6: Trapezoidal rule on a circle

Here and in the next section we derive quadrature formulas for problems with closed contours, beginning with the simplest case of an integral around a circle. If g is an analytic function on the unit circle $\gamma = T = \{z \in \mathbb{C} : |z| = 1\}$, it has a Laurent series

$$g(z) = \sum_{k=-\infty}^{\infty} c_k z^k, \quad c_k = \frac{1}{2\pi i} \oint_T z^{-1-k} g(z)\, dz. \tag{9.1}$$

Since the work of Lyness in the 1960s, it has been recognized that integrals like this can be accurately evaluated by the trapezoidal rule with sample points at the nth roots of unity $\{z_k\}$ for some n (Lyness & Moler, 1967; Lyness & Sande, 1971; Trefethen & Weideman, 2014). For any f analytic on T,

$$\frac{1}{2\pi i} \oint_T f(z)\, dz \approx \sum_{k=1}^{n} \frac{z_k}{n} f(z_k). \tag{9.2}$$

Indeed, this is the standard method for computing Taylor and Laurent coefficients, with adjustments to optimize the radius of the circle of evaluation depending on f (Fornberg, 1981; Bornemann, 2011). For a

review of the history of this technique with many more references, see Austin *et al.* (2014). Applications in numerical linear algebra include many of those cited in the opening paragraph.

For this problem the weight function is $w(z) = (2\pi i)^{-1}$ and the Cauchy transform is

$$2\pi i \mathcal{C}(s) = \begin{cases} -1 & s \text{ interior to } \gamma, \\ 0 & s \text{ exterior to } \gamma. \end{cases} \tag{9.3}$$

Thus $\mathcal{C}(s)$ has a jump of the simplest kind across γ. Let us suppose that f is analytic in the annulus $\Omega = \{z \in \mathbb{C} : \tau^{-1} \le |z| \le \tau\}$ for some $\tau > 1$. (The results will depend little on the choice of τ.) As our enclosing contour Γ of the kind shown on the right in Fig. 1, we take

$$\Gamma = \tau^{-1}T \cup \tau T \tag{9.4}$$

with positive orientation on τT and negative on $\tau^{-1}T$. We now find a degree n rational function r_n that approximates $2\pi i\mathcal{C}$ on Γ as in (2.9). The following code requests an approximation with accuracy 10^{-8}:

```
T = exp(2i*pi*(1:100)'/100);
S = [2*T; 0.5*T];
C = [zeros(size(T)); -ones(size(T))];
[r,pol,res] = aaa(C,S,'tol',1e-8,'sign',1,'lawson',20);
```

The near-best approximation obtained has degree $n = 31$, with 31 poles ranging in modulus from 0.968 to 0.970, plotted on the left in Fig. 13. The phase portrait of $r_n(s) + \frac{1}{2}$, with the constant $\frac{1}{2}$ added to ensure a separation between values $r_n(s) \approx -1$ and $r_n(s) \approx 0$, shows bright cyan in the interior of the disk and bright red in the exterior . To check the accuracy of the approximation as a quadrature formula, we apply it to (9.2) with integrand $f(z) = -2\sqrt{z^2 - 1/4}$, which has a pair of branch points at $z = \pm 1/2$. The computed result `In` is $0.999999999901 + 0.000000000144i$, matching the correct value 1 with an error of about $2 \cdot 10^{-10}$. The exact 31-point trapezoidal rule of (9.2) would improve this just a little bit to $7 \cdot 10^{-11}$.

For the variant problem of this section, shown in Fig. 14, we suppose that it is known that f is analytic not in a circular annulus but in the region of the strip $-1 \le \mathrm{Im} z \le 1$ exterior to the unit interval $[-1, 1]$. One could derive a quadrature formula for this geometry analytically by conformal mapping, but this would take some work, and any modification of the geometry would require a new analysis. Instead we proceed numerically and change the discretization above to

```
segment = linspace(1,1,200)';
long = tan(pi*(-99:99)'/200);
S = [long+1i; long-1i; segment];
C = [zeros(size([long; long])); -ones(size(segment))];
[r,pol,res] = aaa(C,S,'tol',1e-8,'sign',1,'lawson',20);
```

The approximation comes out with degree 40, and we test it on another function with integral 1, $f(z) = -\sqrt{(z-1)/(z+1)}$. The result is $0.999999999956 - 0.000000000024i$ with error $5.0 \cdot 10^{-11}$.

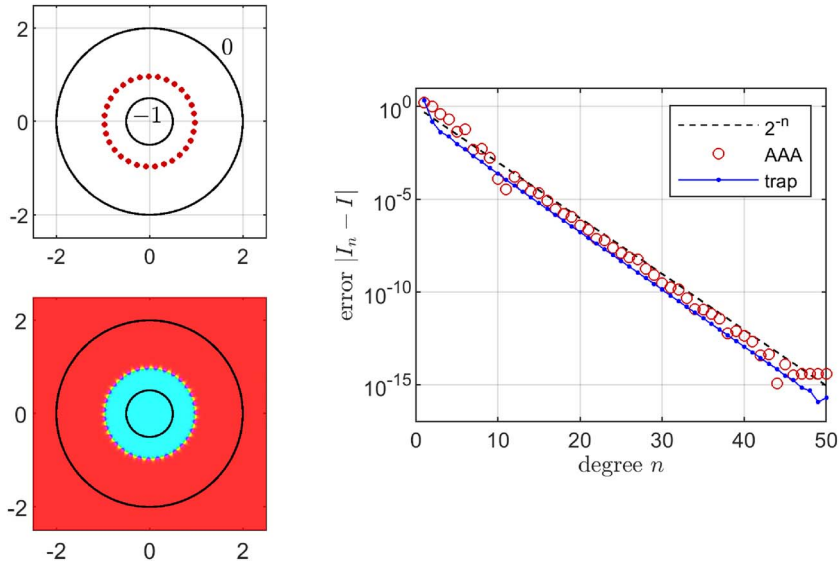

FIG. 13. On the left, quadrature nodes—poles of a degree $n = 31$ rational function—computed in about 0.05 s on a laptop by AAA rational approximation of a two-branch target function with accuracy specification 10^{-8}. The resulting approximate integral (9.2) has accuracy $2 \cdot 10^{-10}$, as compared with $7 \cdot 10^{-11}$ for the exact 31-point trapezoidal rule. The phase portrait now shows $r_n(s) + \frac{1}{2}$ in order to separate values ≈ -1 and ≈ 0. On the right, errors as a function of n.

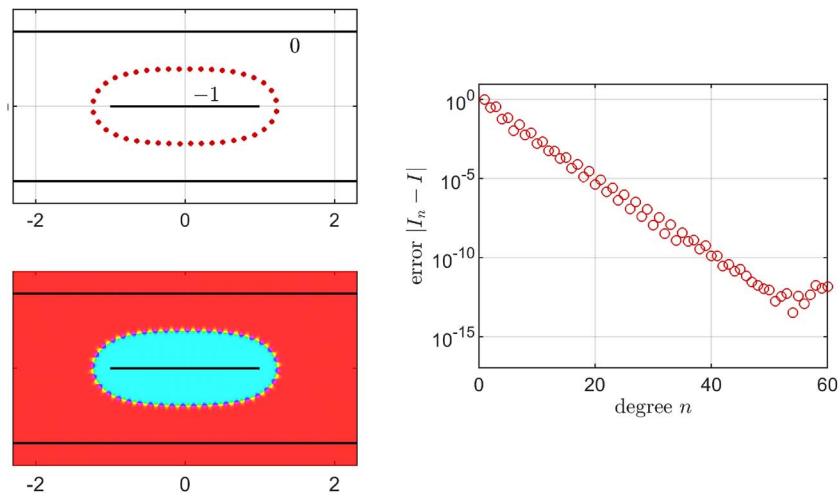

FIG. 14. Repetition of Fig. 13 based on the assumption that f is analytic in the strip $-1 \le \mathrm{Im} z \le 1$ minus the unit interval $[-1, 1]$.

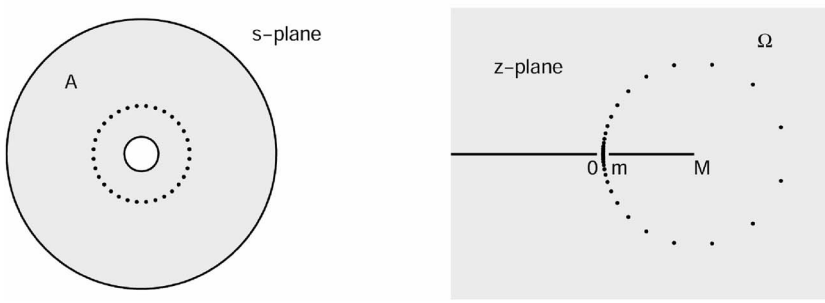

FIG. 15. A figure from Hale *et al.* (2008) showing conformal transplantation of the 32-point equispaced trapezoidal rule in a circular annulus to a domain $\mathbb{C}\backslash\{[m,M]\cup(-\infty,0]\}$ with $m = 1/8$, $M = 1$. This leads to fast evaluation of functions like A^α or $\log(A)$ if A is symmetric positive definite with spectrum contained in $[m,M]$.

10. Application 7: Functions of matrices via Cauchy integrals

A function of a matrix or operator A can be defined by a Cauchy integral (Kato, 1980; Higham, 2008),

$$f(A) = \frac{1}{2\pi i}\int_\Gamma f(z)(zI - A)^{-1}dz, \tag{10.1}$$

where Γ is a closed contour enclosing the spectrum of A and contained in the region of analyticity of f. This suggests the use of discretizations to approximate $f(A)b$ for a given vector b by a linear combination of vectors $(z_kI-A)^{-1}b$, where $\{z_k\}$ are quadrature nodes. For example, suppose A is a symmetric positive definite matrix with eigenvalues in $[m,M]$ for some $0 < m < M < \infty$, as suggested in the right image of Fig. 15, and suppose f is a function like A^α or $\log(A)$ that is analytic in $\mathbb{C}\backslash(-\infty,0]$. Then the trapezoidal rule with n equally spaced points could be applied over a circle passing through the point $z = m/2$, but the convergence as $n\to\infty$ would be very slow, requiring $O(M/m)$ linear solves for each reduction of the error by a constant factor. In the 'three Nicks paper' (Hale *et al.*, 2008), it was shown that this number can be improved enormously to $O(\log(M/m))$ by a conformal map involving Jacobi elliptic functions, as shown in the figure.[3] Now the mathematics is equivalent to the application of the trapezoidal rule on a circular annulus that is conformally equivalent to $\mathbb{C}\backslash\{[m,M]\cup(-\infty,0]\}$. This corresponds to a fast-converging transplanted quadrature formula in unevenly spaced points in the z-plane.

To treat the problem by rational approximation instead of conformal mapping, we note that this is another case where the contour γ is flexible, to be determined, and the Cauchy transform will again be (9.3). Thus, we can adjust the code segment of the last section to

```
segment = logspace(log10(1/8),0,100)';
negreal = 1 - 1./linspace(.005,1,100)';
S = [negreal; segment];
C = [zeros(size(negreal)); -ones(size(segment))];
[r,pol,res] = aaa(C,S,'degree',32,'sign',1,'lawson',0);
```

[3] Zolotarev was an expert in elliptic functions, and the mathematics here is very close to some of his work, though so far as we are aware, he did not make connections between rational approximation and quadrature.

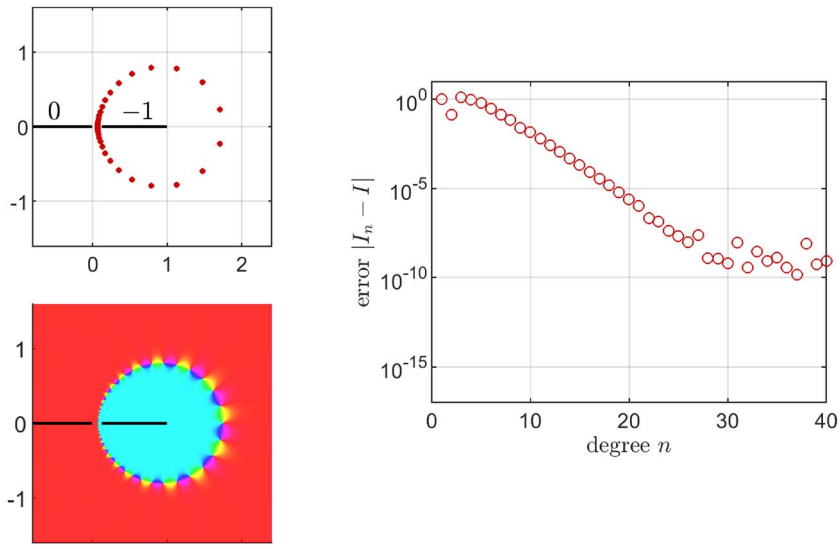

FIG. 16. Treatment of the same problem by rational approximation. On the left, quadrature poles with $n = 32$, giving 8-digit accuracy for a test problem. On the right, convergence for a test problem as a function of n.

The poles shown on the left in Fig. 16 are strikingly similar to those of Fig. 15, even though neither a contour nor a node distribution has been fixed *a priori*. Choosing another integrand with integral exactly 1, $f(z) = (16/7)\sqrt{(z-1/8)/(z-1)}$, gives the result $1.000000000092 - 0.000000000000i$ with error magnitude $9.2 \cdot 10^{-11}$. This problem is more delicate than the last, and for clean results as a function of degree n, shown on the right in Fig. 16, we modified the call to `aaa.m` to

```
[r,pol,res] = aaa(C,S,'degree',n,'sign',1,'lawson',50,'damping',.5);
```

Such adjustments reflect the fact that with the rational approximation algorithms of 2025, hand-tuning is often needed to get the best results. We hope that the situation will improve in the next few years as the algorithms mature.

The variant problem of this section was suggested to us by Maria López-Fernández of the University of Malaga. What if A is not symmetric but is known to have its spectrum in a given region of the right half-plane, like a rectangle? Figure 17 shows that the approximation r now has poles extending much further away from the origin, forming a bend of close to 90° near the spectrum.

11. Quadrature as integration of a rational interpolant

The best-known quadrature formulas, including those of Newton–Cotes, Gauss and Clenshaw–Curtis, are associated with polynomial interpolation. Given a set of n nodes $\{z_k\}$, the weights $\{c_k\}$ are chosen so that the quadrature formula integrates polynomials of degree $n-1$ exactly. Equivalently, the result returned when the formula is applied to a function $f(z)$ is the exact integral of the unique degree $n-1$ polynomial that interpolates $\{f(z_k)\}$ at $\{z_k\}$. This relationship is so familiar that such quadrature formulas are said to be *interpolatory*, even though the logical term would be *polynomial interpolatory*.

The developments of this paper generalize this picture to rational rather than polynomial interpolants. We will describe the construction and then state the result as a theorem. Throughout, we are concerned

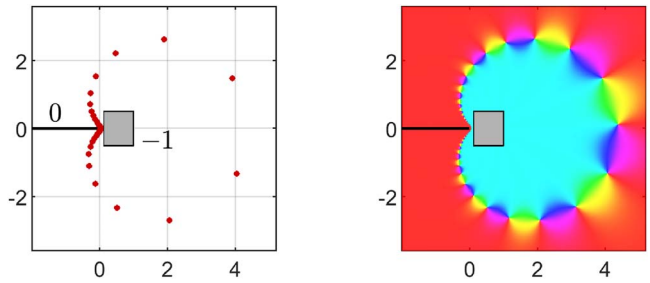

FIG. 17. A variant of Fig. 16 in which the spectrum of A lies in a rectangle.

as in (2.1) with an integral

$$I = \int_\gamma f(z)\, w(z)\, dz \tag{11.1}$$

and as in (2.8) with a quadrature approximation

$$I_n = \sum_{k=1}^{n} c_k f(z_k) \tag{11.2}$$

defined by nodes $z_1, \ldots, z_n$ and weights $c_1, \ldots, c_n$. The nodes may or may not lie exactly on γ. If not, we assume that f is analytic in a neighborhood of γ that includes $\{z_k\}$, so that $f(z_k)$ is defined by analytic continuation. We let $\mathcal{C}(s)$ denote the Cauchy transform (2.4) of $w(z)$ with respect to γ.

The construction involves two different rational functions. One of them, r_n, has been discussed throughout this paper:

The Cauchy interpolant $r_n(s)$. This is a rational function (2.7) of degree at most n with poles $z_1, \ldots, z_n$ and residues $c_1, \ldots, c_n$. (The degree is less than n if one or more residues are zero.) These conditions determine $r_n(s)$ apart from the constant $c_\infty = r_n(\infty)$, which does not matter much since it does not appear in (11.2). (The number c_∞ still has some interest since it will affect (2.9) and thereby (2.10); in practice c_∞ will usually be close to zero. See the note at the end of this section regarding the condition $r_n(\infty) = 0$.) For what follows we assume that $r_n(s)$ interpolates $2\pi i \mathcal{C}(s)$ at $n+1$ points $s_0, \ldots, s_n \in (\mathbb{C} \cup \{\infty\})\backslash\gamma$, which need not be distinct and need not be finite. Typically, there will actually be more than $n+1$ points of interpolation, generically $2n+1$ or more for best or near-best approximations, in which case any $n+1$ of them can be selected as $s_0, \ldots, s_n$. The same weights $\{c_k\}$ are determined by these $n+1$ interpolation conditions, regardless of which points $s_0, \ldots, s_n$ are selected.

The other rational function, which we have not introduced until now, is the implicit interpolant:

The quadrature interpolant $q_{n+1}(z)$. This is a rational function of degree at most $n+1$ with poles at each of the points $s_0, \ldots, s_n$ that are finite (again a pole may be absent if a residue turns out to be zero), and which interpolates f at $z_1, \ldots, z_n$. If the numbers $\{s_k\}$ are all finite, then $q_{n+1}(z)$ is defined uniquely by additionally having a double zero at $z = \infty$. If one of these numbers is ∞, then q_{n+1} is determined by being of degree at most n and having a zero of order 1 at ∞, and if $\nu \geq 2$ of them are ∞, then q_{n+1} is determined by being of degree at most $n-1$ and having a pole of order at most $\nu - 2$ at ∞.

Note the elegant duality in these definitions. Apart from the complication at $z = \infty$, the poles of r_n are the interpolation points of q_{n+1} ($q_{n+1}(z_k) = f(z_k)$), and the poles of q_{n+1} are the interpolation points of r_n ($r_n(s_k) = \mathcal{C}(s_k)$).

Our theorem asserts that the quadrature formula implicitly integrates this quadrature interpolant.

THEOREM 11.1. Let a quadrature formula (11.2) be defined by nodes $z_1, \ldots, z_n$, weights $c_1, \ldots, c_n$ and interpolation of the Cauchy transform of $w(z)$ on γ at any $n+1$ points $s_0, \ldots, s_n$ as described above. Then the formula integrates any rational function of the class defined above exactly. Specifically, the result returned when the formula is applied to an integrand $f(z)$ is the exact integral of the quadrature interpolant defined above to the data $\{f(z_k)\}$:

$$I_n = \int_\gamma q_{n+1}(z)\, w(z)\, dz. \tag{11.3}$$

Proof. Let q_{n+1} be a rational function of the indicated class, and in the notation of section 2, let Γ be a contour enclosing γ but excluding $s_0, \ldots, s_n$. From (2.5) and (2.6), we have

$$I_n - I = \frac{1}{2\pi i} \int_\Gamma q_{n+1}(s) \big[r_n(s) - 2\pi i \mathcal{C}(s) \big] ds. \tag{11.4}$$

Now this integrand is analytic on and exterior to Γ in $\mathbb{C}$, except potentially at the poles of $q_{n+1}(s)$. By definition, however, these are canceled by zeros of $r_n(s) - 2\pi i \mathcal{C}(s)$. Thus, the integrand is analytic everywhere exterior to Γ, and we can deform the contour of integration out toward ∞. Suppose first that all the numbers $s_0, \ldots, s_n$ are finite. Then by the construction of q_{n+1}, $q_{n+1}(s) = O(|s|^{-2})$ as $|s| \to \infty$, so by the usual estimate for Cauchy integrals over large contours, the integral must be zero. Next, if one of the numbers is ∞ then $q_{n+1}(s) = O(|s|^{-1})$ as $|s| \to \infty$ and another order of decay is provided by $r_n(s) - 2\pi i \mathcal{C}(s)$ since this difference is zero at $s = \infty$. Finally, if $\nu \geq 2$ of the numbers are ∞, then $r_n(s) - 2\pi i \mathcal{C}(s) = O(|s|^{-\nu})$, whereas $q(z) = O(|s|^{\nu-2})$ as $|s| \to \infty$, so the product is $O(|s|^{-2})$ and once more the integral is zero. □

Theorem 11.1 reduces to a description of polynomial interpolatory quadrature when the quadrature interpolant q_{n+1} has all its poles at ∞, so that it is a polynomial of degree $n-1$. In this case the Cauchy interpolant r_n is the unique degree n rational function with poles at $z_1, \ldots, z_n$ that matches the Taylor series of $\mathcal{C}(s)$ through order n at $s = \infty$. In the case of Gauss quadrature, r_n is the degree n Padé approximant of $\mathcal{C}(s)$ at $s = \infty$, interpolating there all the way through order $2n$. For Clenshaw–Curtis quadrature, the interpolation at $s = \infty$ is only through order n, and there are n additional points of interpolation on an approximately elliptical curve near $[-1, 1]$, as investigated in Gauss (1814).

There is a further comment to be made about the condition $r_n(\infty) = 0$ mentioned above and in Section 2. For many applications it may make good sense to impose this condition exactly, and when one does, the duality of rational functions described in this section becomes more perfect. The factor $r_n(s) - 2\pi i \mathcal{C}(s)$ of (11.4) is now of size $O(|s|^{-1})$ as $|s| \to \infty$, which means that q_{n+1} no longer needs to do as much work and can be replaced by a rational function q_n of degree n with just a single zero at ∞.

12. Discussion

Nothing is entirely new in the field of quadrature, and the link with rational functions starts with Gauss (1814) and has been exploited in many ways since then. Most of this work has been algebraic, however,

related to Padé approximations at ∞ and associated orthogonal polynomials. The present paper has followed a more analytic approach based on numerical rational approximations made possible by the AAA algorithm. Here there is a smaller tradition, including the contributions (Takahasi & Mori, 1971; Trefethen *et al.*, 2006; Trefethen, 2008).

Whenever you see a string of quadrature nodes, you should consider it as a rational approximation to a branch cut. That is our conceptual message. Our practical message is that it is amazingly easy to compute near-optimal quadrature formulas by taking advantage of this connection. We make no claim that any of the particular techniques we have illustrated will immediately bring improvements in computational science, but we have outlined many possibilities and are confident that some of them will prove useful.

Jumps of complex functions across arcs arise in many contexts and are associated with notions including Cauchy/Stieltjes/Hilbert transforms, the Sokhotski–Plemelj formula, Wiener–Hopf factorization, the Dirichlet-to-Neumann map and Riemann–Hilbert problems (Nakatsukasa & Trefethen, 2025). The literature of such topics is enormous, and links could be found from this paper to most of it. Another topic in this space is that of *hyperfunctions*, which are generalized functions realized as (equivalence classes of) pairs of analytic functions on either side of an arc (Graf, 2010). The present paper could be said to investigate quadrature formulas as rational hyperfunction approximations to Cauchy transforms. Perhaps this work can help encourage the growth of a numerical theory of hyperfunctions, which has been mostly a theoretical topic heretofore.

Theoretical questions lie around every corner. Exactly what are the links with potential theory? Does the phenomenon of 'balayage' (Saff & Totik, 1997; Gustafsson, 2001) relate interpolation points at ∞, for example, to almost equally effective points along a Bernstein ellipse? Can backward error analysis confirm our experience that nodes and weights may be individually far from optimal yet still combine to give nearly optimal quadratures? Can one prove in some generality that best rational approximations match the convergence rates of Gauss quadrature rules? When can weights (= residues) be guaranteed to be positive, or at least uniformly summable as $n \to \infty$? These are just a few examples of many problems to be explored.

Acknowledgements

We are grateful for helpful suggestions from Matt Colbrook, Toby Driscoll, Stefan Güttel, Nick Hale, Arno Kuijlaars, Maria López-Fernández, Yuji Nakatsukasa, Sheehan Olver, Mikaël Slevinsky, Tom Trogdon, Kieran Vlahakis, André Weideman and Heather Wilber. In particular, the ideas of Section 11 were worked out in discussion with Vlahakis. We have also benefited from the constructive comments of two anonymous referees.

References

Austin, A. P., Kravanja, P. & Trefethen, L. N. (2014) Numerical algorithms based on analytic function values at roots of unity. *SIAM J. Numer. Anal.*, **52**, 1795–1821.

Bakhvalov, N. S. (1967) On the optimal speed of integrating analytic functions. *Comput. Math. Math. Phys.*, **7**, 63–75.

Beyn, W.-J. (2012) An integral method for solving nonlinear eigenvalue problems. *Lin. Alg. Appl.*, **436**, 3839–3863.

Bornemann, F. (2011) Accuracy and stability of computing high-order derivatives of analytic functions by Cauchy integrals. *Found. Comput. Math.*, **11**, 1–63.

Brennan, M. C., Embree, M. & Gugercin, S. (2023) Contour integral methods for nonlinear eigenvalue problems: A systems theoretic approach. *SIAM Rev.*, **65**, 439–470.

Bruno, O. P., Santana, M. A. & Trefethen, L. N. (2024) Evaluation of resonances: Adaptivity and AAA rational approximation of randomly scalarized boundary integral resolvents. *SIAM J. Sci. Comput.*, submitted for publication.

Chandler-Wilde, S. N., Graham, I. G., Langdon, S. & Spence, E. A. (2012) Numerical-asymptotic boundary integral methods in high-frequency acoustic scattering. *Acta Numerica*, **21**, 89–305.

Colbrook, M. J. (2022) Computing semigroups with error control. *SIAM J. Numer. Anal.*, **60**, 396–422.

Colbrook, M. J. & Townsend, A. (2025) Avoiding discretization issues for nonlinear eigenvalue problems. *SIAM J. Matrix Anal. Appl.*, **46**, 648–675.

Deaño, A. & Huybrechs, D. (2009) Complex Gaussian quadrature of oscillatory integrals. *Numer. Math.*, **112**, 197–219.

Deaño, A., Huybrechs, D. & Iserles, A. (2017) *Computing Highly Oscillatory Integrals*. Philadelphia, PA: Society for Industrial and Applied Mathematics.

Driscoll, T. A. (2023) *RationalFunctionApproximation.Jl: Approximation by Rational Functions on Intervals and Domains in the Complex Plane (Version*0.1.0*) [Computer Software]*. https://doi.org/10.5281/zenodo.8355791.

Driscoll, T. A., Hale, N. & Trefethen, L. N. (2014) *Chebfun User's Guide*. Oxford: Pafnuty Publications. Available at www.chebfun.org.

Driscoll, T. A., Nakatsukasa, Y. & Trefethen, L. N. (2024) AAA rational approximation on a continuum. *SIAM J. Sci. Comput.*, **46**, A929–A952.

Driscoll, T. A. & Zhou, Y. (2025) Greedy Thiele continued-fraction approximation on continuum domains in the complex plane. arXiv preprint arXiv:2510.07295. Accessed 21 April, 2026.

El-Guide, M., Miedlar, A. & Saad, Y. (2020) A rational approximation method for solving acoustic nonlinear eigenvalue problems. *Eng. Anal. Bound. Elem.*, **111**, 44–54.

Filon, L. N. G. (1930) On a quadrature formula for trigonometric integrals. III. *Proc. Roy. Soc. Edinburgh*, **49**, 38–47.

Fornberg, B. (1981) Numerical differentiation of analytic functions. *ACM Trans. Math. Softw.*, **7**, 512–526.

Gauss, C. F. (1814) Methodus nova integralium valores per approximationem inveniendi. *Comment. Soc. Reg. Scient. Gotting. Recent.*, 39–76.

Gautschi, W. (1981) *A survey of Gauss–Christoffel quadrature formulae*. *E. B. Christoffel: The Influence of his Work in Mathematics and the Physical Sciences* (P. L. Butzer & F. Fehér eds.). Birkhäuser, pp. 72–147.

Gautschi, W. (2004) *Orthogonal Polynomials: Computation and Approximation*. Oxford: Oxford University Press.

Goedecker, S. (1999) Linear scaling electronic structure methods. *Rev. Modern Phys.*, **71**, 1085–1123.

Graf, U. (2010) *Introduction to Hyperfunctions and their Integral Transforms: An Applied and Computational Approach*. Basel: Birkhäuser.

Gustafsson, B. (2001) Lectures on Balayage. *U. Joensuu, Dept. Rep. Ser*.

Güttel, S., Polizzi, E., Tang, P. T. P. & Viaud, G. (2015) Zolotarev quadrature rules and load balancing for the FEAST eigensolver. *SIAM J. Sci. Comput.*, **37**, A2100–A2122.

Güttel, S. & Tisseur, F. (2017) The nonlinear eigenvalue problem. *Acta Numerica*, **26**, 1–94.

Hale, N., Higham, N. J. & Trefethen, L. N. (2008) *Computing* A^{α}, $\log(A)$*, and related matrix functions by contour integrals*. *SIAM J. Numer. Anal.*, **46**, 2505–2523.

Hale, N. & Tee, T. W. (2009) Conformal maps to multiply slit domains and applications. *SIAM J. Sci. Comput.*, **31**, 3195–3215.

Hale, N. & Trefethen, L. N. (2008) New quadrature formulas from conformal maps. *SIAM J. Numer. Anal.*, **46**, 930–948.

Higham, N. J. (2008) *Functions of Matrices: Theory and Computation*. Philadelphia: Society for Industrial and Applied Mathematics.

Horning, A. & Gerlach, A. R. (2024) A family of high-order accuracy contour integral methods for strongly continuous semigroups. arXiv:2408.07691. Accessed 21 April, 2027.

Huybrechs, D. & Vandewalle, S. (2006) On the evaluation of highly oscillatory integrals by analytic continuation. *SIAM J. Numer. Anal.*, **44**, 1026–1048.

Iserles, A., Nørsett, S. P. & Olver, S. (2006) Highly oscillatory quadrature: the story so far. *Numerical Mathematics and Advanced Applications: Proceedings of ENUMATH 2005*. Santiago de Compostela, Spain: Springer, pp. 97–118.

Istace, M.-P. & Thiran, J.-P. (1995) On the third and fourth Zolotarev problems in the complex plane. *SIAM J. Numer. Anal.*, **32**, 249–259.

Kato, T. (1980) *Perturbation Theory for Linear Operators*, 2nd edn. Berlin: Springer.

Klöckner, A., Barnett, A., Greengard, L. & O'Neil, M. (2013) Quadrature by expansion: a new method for the evaluation of layer potentials. *J. Comput. Phys.*, **252**, 332–349.

Kosloff, D. & Tal-Ezer, H. (1993) A modified Chebyshev pseudospectral method with an $O(N^{-}1)$ time step restriction. *J. Comp. Phys.*, **104**, 457–469.

Levin, D. (1982) Procedures for computing one- and two-dimensional integrals of functions with rapid irregular oscillations. *Math. Comp.*, **38**, 531–538.

López-Fernández, M., Palencia, C. & Schädle, A. (2006) A spectral order method for inverting sectorial Laplace transforms. *SIAM J. Numer. Anal.*, **44**, 1332–1350.

Lyness, J. N. & Moler, C. B. (1967) Numerical differentiation of analytic functions. *SIAM J. Numer. Anal.*, **4**, 202–210.

Lyness, J. N. & Sande, G. (1971) Algorithm 413: ENTCAF and ENTCRE: evaluation of normalized Taylor coefficients of an analytic function. *Commun. ACM*, **14**, 669–675.

MathWorks (2024) *RF Toolbox*. Natick, Massachusetts, USA: Well it's MathWorks, Inc. Available at www.mathworks.com.

Nakatsukasa, Y., Sète, O. & Trefethen, L. N. (2018) The AAA algorithm for rational approximation. *SIAM J. Sci. Comput.*, **40**, A1494–A1522.

Nakatsukasa, Y. & Trefethen, L. N. (2020) An algorithm for real and complex rational minimax approximation. *SIAM J. Sci. Comput.*, **42**, A3157–A3179.

Nakatsukasa, Y. & Trefethen, L. N. (2025) Applications of AAA rational approximation. *Acta Numerica*, Submitted for publication.

Polizzi, E. (2009) Density-matrix-based algorithm for solving eigenvalue problems. *Phys. Rev. B*, **79**, 115112-1–115112-6.

Rakhmanov, E. A. (2016) The Gonchar–Stahl ρ^2-theorem and associated directions for studies on rational approximations of analytic functions. *Sb. Math.*, **207**, 1236–1266.

Saff, E. B. & Totik, V. (1997) *Logarithmic Potentials with External Fields*. Berlin, Heidelberg: Springer.

Sakurai, T. & Sugiura, H. (2003) A projection method for generalized eigenvalue problems using numerical integration. *J. Comput. Appl. Math.*, **159**, 119–128.

Salazar Celis, O. (2024) Numerical continued fraction interpolation. *Ukrainian Math. J.*, **76**, 568–580.

Silver, R. N., Roeder, H., Voter, A. F. & Kress, J. D. (1996) Kernel polynomial approximations for densities of states and spectral functions. *J. Comput. Phys.*, **124**, 115–130.

Stahl, H. (1997) The convergence of Padé approximants to functions with branch points. *J. Approx. Theory*, **91**, 139–204.

Takahasi, H. & Mori, M. (1971) Estimation of errors in the numerical quadrature of analytic functions. *Appl. Anal.*, **1**, 201–229.

Tee, T. W. & Trefethen, L. N. (2006) A rational spectral collocation method with adaptively transformed Chebyshev grid points. *SIAM J. Sci. Comput.*, **28**, 1798–1811.

Trefethen, L. N. (2008) Is Gauss quadrature better than Clenshaw–Curtis? *SIAM Rev.*, **50**, 67–87.

Trefethen, L. N. (2019) *Approximation Theory and Approximation Practice, Extended Ed.* Philadelphia: Society for Industrial and Applied Mathematics.

Trefethen, L. N. (2022) Exactness of quadrature formulas. *SIAM Rev.*, **64**, 132–150.

Trefethen, L. N. (2025) Rational approximation. *Notices AMS*, **72**, 78–81.

Trefethen, L. N. & Weideman, J. A. C. (2014) The exponentially convergent trapezoidal rule. *SIAM Rev.*, **56**, 385–458.

Trefethen, L. N., Weideman, J. A. C. & Schmelzer, T. (2006) Talbot quadratures and rational approximations. *BIT Numer. Math.*, **46**, 653–670.

Trefethen, L. N. & Wilber, H. D. (2025) Computation of Zolotarev rational functions. *SIAM J. Sci. Comput.*, **47**, A2205–A2220.

Van Hove, L. (1953) The occurrence of singularities in the elastic frequency distribution of a crystal. *Phys. Rev.*, **89**, 1189–1193.

Virtanen, P., Gommers, R., Oliphant, T. E., Haberland, M., Reddy, T., Cournapeau, D., Burovski, E., Peterson, P., Weckesser, W., Bright, J., van der Walt, S., Brett, M., Wilson, J., Millman, K. J., Mayorov, N., Nelson, A. R. J., Jones, E., Kern, R., Larson, E., Carey, C. J., Polat, İ., Feng, Y., Moore, E. W., VanderPlas, J., Laxalde, D., Perktold, J., Cimrman, R., Henriksen, I., Quintero, E. A., Harris, C. R., Archibald, A. M., Ribeiro, A. H., Pedregosa, F., van Mulbregt, P. & SciPy 1.0 Contributors (2020) SciPy 1.0: Fundamental algorithms for scientific computing in Python. *Nat. Methods*, **17**, 261–272.

Wallace, P. R. (1947) The band theory of graphite. *Phys. Rev.*, **71**, 622–634.

Wegert, E. (2012) *Visual Complex Functions: An Introduction with Phase Portraits*. Basel: Springer.

Weideman, J. A. C. & Trefethen, L. N. (2007) Parabolic and hyperbolic contours for computing the Bromwich integral. *Math. Comp.*, **76**, 1341–1356.

Weisse, A., Wellein, G., Alvermann, A. & Fehske, H. (2006) The kernel polynomial method. *Rev. Modern Phys.*, **78**, 275–306.